ULTRASONIC MONITORING OF RECRYSTALLIZATION TEXTURES IN ALUMINUM

G. Liu, F. Laabs, D. Rehbein, O. Buck, and R.B. Thompson

Ames Laboratory
Iowa State University
Ames, Iowa 50011

INTRODUCTION

The present paper is an attempt to use ultrasonic velocity measurements to characterize the texture of an aluminum-magnesium alloy (Al 5xxx) and to compare the results with orientation imaging microscopy (OIM) results. The results are characterized in terms of three orientation distribution coefficients (ODC's), W_{400} , W_{420} , and W_{440} , each of which describes a particular forming anisotropy, and each of which has significant impact on the final products.

We took the following steps. The as-received material was fully characterized (OIM and ultrasonic velocity measurement) yielding a weak (001)[100] cube texture. The two techniques provided quantitatively very similar ODC's. We then continued to cold roll the specimens to about 20, 50, or 80% thickness reduction, respectively, following the change of the ODC's ultrasonically. Each one of the severely cold rolled samples was then recrystallized and the ODC's determined as far as possible. We provide information on the textures that have been achieved with each step and come to the conclusion that ultrasonic measurements provide a promising approach to follow the development of texture of one of the basic manufacturing processes[1] that may even lend itself to numerical solution [2-4]. It appears that ultrasonics is a relatively quick and precise method, so that field applications [5,6] should be possible with the mathematical tools given in this present paper.

ORIENTATION DISTRIBUTION COEFFICIENTS AND ULTRASONIC VELOCITIES

The most convenient representation of the texture is the pole figure[7,8], which can be used to obtain a quantitative crystallite orientation distribution function using the method of Roe[9]. The crystallite orientation distribution function, $W(\xi, \psi, \phi)$, which expresses the probability of a crystallite having an orientation described by the Euler angles (θ,ψ,ϕ), can be expressed by

Review of Progress in Quantitative Nondestructive Evaluation, Vol. 17
Edited by D.O. Thompson and D.E. Chimenti,, Plenum Press, New York, 1998

$$W(\xi,\psi,\phi)=\sum_{l=0}^{\infty}\sum_{m=-l}^{l}\sum_{n=-l}^{l}W_{lmn}Z_{lmn}(\xi)\exp(-im\psi)\exp(-in\phi) \quad (1)$$

where $\xi=\cos(\theta)$. Here the Z_{lmn} are generalized Legendre functions, and the expansion coefficients, W_{lmn}, are known as orientation distribution coefficients (ODC's).

The number of ODC's for general determination of the texture is theoretically infinite. However, owing to the symmetric requirements of the cubic system and the relative magnitude of ODC's, only a few ODC's are of practical interest. It is known that the ODC's are related to the earring behavior of the materials[5, 10, 11], i.e., W_{400} sets the overall value of the average strain ratio; W_{420} controls the tendency to form two ears during deep drawing while W_{440} controls the tendency to form four ears.

Recent theoretical developments have allowed a quantitative prediction of the effect of texture on ultrasonic velocities[5,12-15]. The elastic constants, C_{ii} (i=1,2, ..., 6) are related to the ultrasonic velocities by

$$\rho V_{11}^2 = C_{11} \quad (2a)$$
$$\rho V_{22}^2 = C_{22} \quad (2b)$$
$$\rho V_{33}^2 = C_{33} \quad (2c)$$
$$\rho V_{12}^2 = \rho V_{21}^2 = C_{66} \quad (2d)$$
$$\rho V_{13}^2 = \rho V_{31}^2 = C_{55} \quad (2f)$$
$$\rho V_{23}^2 = \rho V_{32}^2 = C_{44} \quad (2g)$$

where ρ is the density of the material. V_{ii} is the longitudinal ultrasonic propagation velocity along the ith direction. V_{ij} is the shear wave velocity propagating in the ith direction polarized in the jth direction. Theoretically, $V_{ij} = V_{ji}$ (i, j =1,2,3, which represents rolling, transverse, and normal direction, respectively).

The ODC's can be obtained by solving the following equations[12].

$$C_{11}=\lambda+2\mu+\frac{12\sqrt{2}C^o}{35}\pi^2\left[W_{400}-\frac{2\sqrt{10}}{3}W_{420}+\frac{\sqrt{70}}{3}W_{440}\right] \quad (3a)$$

$$C_{22}=\lambda+2\mu+\frac{12\sqrt{2}C^o}{35}\pi^2\left[W_{400}+\frac{2\sqrt{10}}{3}W_{420}+\frac{\sqrt{70}}{3}W_{440}\right] \quad (3b)$$

$$C_{33}=\lambda+2\mu+\frac{12\sqrt{2}C^o}{35}\pi^2 W_{400} \quad (3c)$$

$$C_{12}=\lambda+\frac{4\sqrt{2}C^o}{35}\pi^2\left[W_{400}-\sqrt{70}W_{440}\right] \quad (3d)$$

$$C_{13}=\lambda-\frac{16\sqrt{2}C^o}{35}\pi^2\left[W_{400}-\sqrt{\frac{5}{2}}W_{420}\right] \quad (3e)$$

$$C_{23} = \lambda - \frac{16\sqrt{2}C^o}{35}\pi^2\left[W_{400} + \sqrt{\frac{5}{2}}W_{420}\right] \quad (3f)$$

$$C_{44} = \mu - \frac{16\sqrt{2}C^o}{35}\pi^2\left[W_{400} + \sqrt{\frac{5}{2}}W_{420}\right] \quad (3g)$$

$$C_{55} = \mu - \frac{16\sqrt{2}C^o}{35}\pi^2\left[W_{400} - \sqrt{\frac{5}{2}}W_{420}\right] \quad (3h)$$

$$C_{66} = \mu + \frac{4\sqrt{2}C^o}{35}\pi^2\left[W_{400} - \sqrt{70}W_{440}\right] \quad (3i)$$

$$C^o = C^o_{11} - C^o_{12} - 2C^o_{44} \quad (3j)$$

where λ and μ are the macroscopic Lamé constants of the isotropic aggregate when the crystallites are randomly oriented. C^o_{11}, C^o_{12}, and C^o_{44} are the elastic constants of the single crystal[16].

For our aluminum alloy, we used the C^o value of pure aluminum in Eqns. 3 to calculate ODC's. The Lamé constants were determined by the following equations

$$\mu = \rho V_T^2 \quad (4a)$$

$$\lambda = \rho(V_L^2 - 2V_T^2) \quad (4b)$$

where V_T is the shear wave velocity of the isotropic sample and V_L is the longitudinal wave velocity of the isotropic sample. The isotropic sample was prepared by annealing the aluminum alloy sample. After measuring the ultrasonic velocities, we calculated the Lamé constants by Eqns. (4). The density was calculated by measuring the weight and the sizes of the samples. We obtained the following materials constants from which we calculated the ODC's. Included is C^o which we obtained from Ref. [16].

ρ = 2.65 g/cm^3
μ =26.74 GPa
λ =54.91 GPa
C^o=-10.77 GPa

SAMPLES AND EXPERIMENT

We have used fourteen samples in this study all of them taken from the same sheet of 5xxx aluminum alloy (Al-Mg) in the as-received condition. The sheet was cold rolled in-house to different thickness reductions, and then aged at different aging temperatures and holding time combinations.

The texture measurements have been taken by using both the ultrasonic technique and orientation imaging microscopy which is a new technique using the electron back-scatter diffraction patterns to obtain local lattice orientation information[17]. For each ultrasonic measurement, there are three repetitions and the average value is used in the final computation.

RESULTS AND DISCUSSIONS

Using orientation imaging microscopy, the pole figures can be obtained. Figure 1 below shows the texture in the as-received condition. One can see that the texture has a mild cube component, evidenced by the four spots of high intensity at [100], [010], etc. This was the material's starting texture before cold rolling and aging. This cube texture is typical for the recrystallization texture component in pure aluminum.

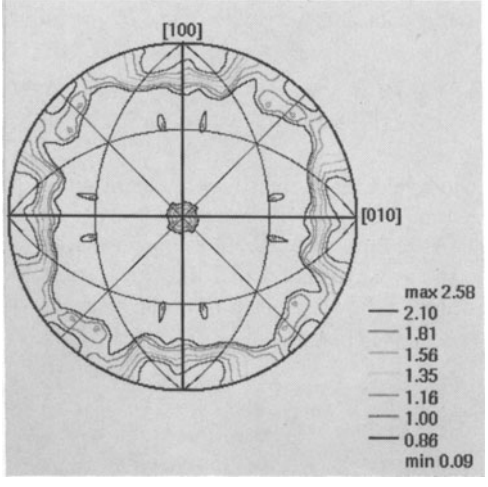

Fig. 1 Inverse pole figure of the as-received sample.

When the sample was cold rolled to 50% thickness reduction, the inverse pole figure as shown in Figure 2 below is more informative. It is obvious that the new texture then has components which are totally different from the cube component shown in Figure 1. Therefore, the texture will change from recrystallization texture to a new cold rolling texture when the samples are cold rolled to high thickness reduction.

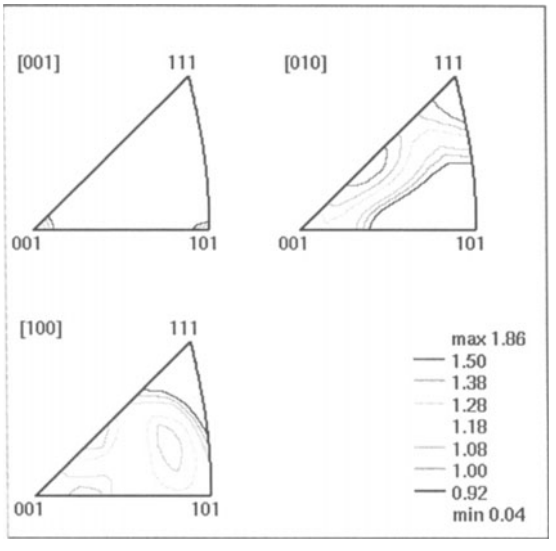

Fig.2 Inverse pole figure of 50% thickness reduction sample.

Acoustic ODC's have been obtained from Eqns. 3 by different routes. In order to calculate the ODC's with a minimum of experimental error, we used a Taylor expansion method to obtain Equations (5) and (6) from Equations (2c, 2e, 2f) and (3c, 3g, 3h), and chose to form sums and differences of Equations (3g, 3h, 3i) to arrive at Equation (7):

$$W400 \cong \frac{\lambda+2\mu}{\lambda+4\mu} \quad \frac{35\sqrt{2}\mu}{16C^{o}\pi^{2}} \quad \left[\frac{V33}{V31+V32}\left(\frac{4\mu}{\lambda+2\mu}\right)^{1/2}-1\right] \tag{5}$$

$$W420 \cong \frac{35\sqrt{5}}{40\pi^{2}} \quad \frac{\mu}{C^{o}} \quad \frac{V31-V32}{V31+V32} \tag{6}$$

$$W440 = \frac{\sqrt{35}}{8C^{o}\pi^{2}} \quad \left[\frac{C44+C55}{2}-C66\right]+\frac{5\sqrt{70}}{2}W400 \tag{7}$$

The progression of the acoustic ODC's as a function of thickness reduction and aging are shown in Figures 3~5 below. From Figure 3, one can see that when the thickness reduction increases, ODC's decrease but the change of W_{420} is complicated. During the aging process, the rolling texture will again change to a recrystallization texture. This is affirmed by Figures 4 and 5. The higher the aging temperature, the faster the recrystallization process. For example, when the 80% thickness reduction sample was aged at 350°C, ODC's changed from negative to positive values, i.e., the texture changed from rolling texture to recrystallization texture in less than 5 hours. Unfortunately, when the thickness reduction is very large, the small dimension of samples makes it difficult to

measure W_{440} with reasonable precision by ultrasonic techniques. Thus, Figures 4 and 5 do not show W_{440}.

Table 1 lists the ideal texture in pure aluminum and Table 2 lists the ODC's measured by Los Alamos Laboratory[18] and our results. Comparing the acoustic and OIM ODC's of the as-received sample, one can see that they agree quite well with each other (Table 2). The measured ODC's (Table 2) of the as-received sample are close to but much less in value than those of the cube recrystallization texture (Table1), which means that the material's starting texture has a weak cube component. This result is consistent with the orientation microscopy result (Figure 1). When the thickness reduction is 80%, the measured ODC's values (Table 2) are close to those of the B_r rolling texture component (Table 1), i.e., the rolling texture appears. After 350^0C aging, the ODC values of the 80% thickness reduction sample (Table 2) come back again close to those of the cube component.

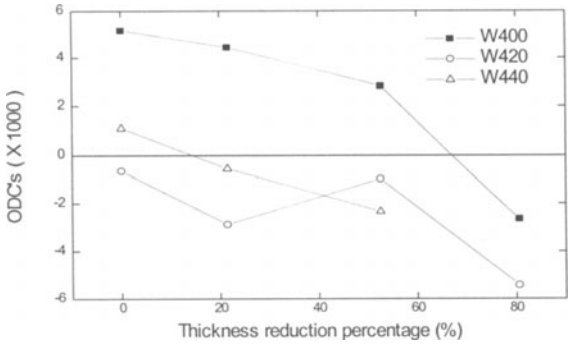

Fig. 3 ODC's vs cold rolling percentage (without aging).

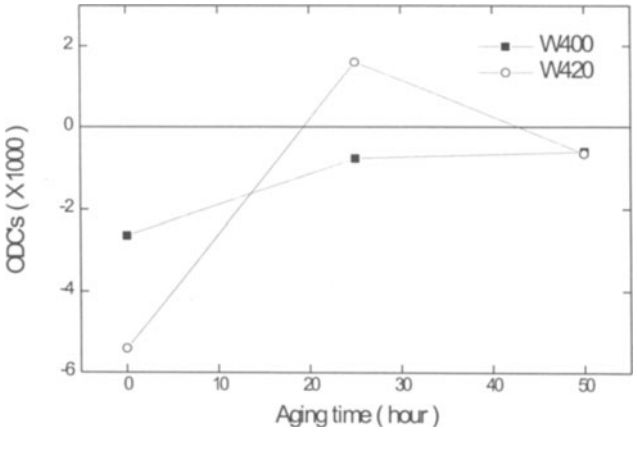

Fig. 4 ODC's vs aging time (80.6% thickness reduction and 310C aging).

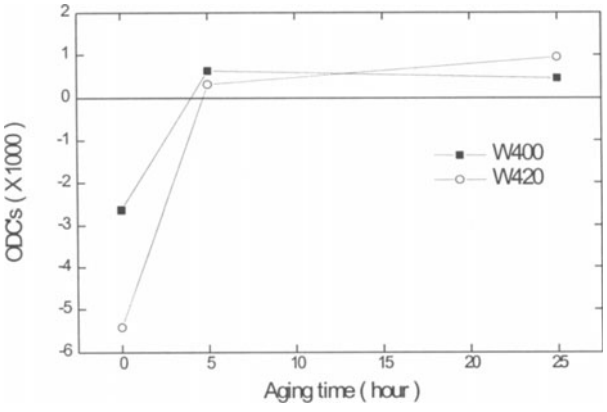

Fig. 5 ODC's vs aging time (80.6% thickness reduction and 350C aging).

Table 1. Ideal pure aluminum texture, (10^{-3}), based on [19].

Texture	W_{400}	W_{420}	W_{440}	Type of texture
Goss{110}<001>	-7.7	-24.4	13.4	Recrystallization
Cube{100}<001>	30.9	0.0	18.5	Recrystallization
Cu{112}<11$\bar{1}$>	-7.7	8.1	-10.8	Rolling
S{123}<63$\bar{4}$>	-7.7	-0.3	-8.9	Rolling
Br{110}<$\bar{1}$12>	-7.7	-8.1	-10.8	Rolling

Table 2 Comparison of acoustic ODC's and OIM ODC's[18] of as received mateials. The effect of further cold rolling and aging on the acoustic ODC's is also shown, (10^{-3}).

	W_{400}	W_{420}	W_{440}	Sample condition
Acoust. ODC's	5.18	-0.64	1.11	As-received sample
Acoust. ODC's	-2.64	-5.42	N/A	80% cold rolled
Acoust. ODC's	0.46	0.95	N/A	80% cold rolled+350C aging
OIM ODC's[18]	4.34	0.21	0.24	As-received sample

SUMMARY AND CONCLUSION

We have shown in this paper that the texture in an as received aluminum alloy 5xxx can be inferred from ultrasonic velocity measurements. The materials starting texture studied has a weak cube component. When the thickness reduction percentage is increased to 80%, the rolling texture becomes the main component. As the cold rolled samples are

aged, the recrystallization process changes from the rolling texture back to a recrystallization texture. The higher the aging temperature, the faster the recrystallization process. The ODC's measured by Los Alamos[18] and us using two different techniques agree very well. The orientation imaging microscopy technique is used to analyze the texture in the samples, which confirms the ultrasonic measurement results.

ACKNOWLEDGMENT

Ames Laboratory is operated for the US Department of Energy by Iowa State University under Contract W-7405-ENG-82. This work was supported by the Office of Basic Energy Sciences as a part of the Center of Excellence of the Synthesis and Processing of Advanced Materials.

REFERENCES

1. Kalpakjian, S., Manufacturing Processes for Engineering Materials, Addison-Wesley: Reading, MA, 1997.
2. R.W. Evan, in Mathematical Modeling for Materials Processing, ed. M. Cross, J.F.T. Pittman, and R.D. Wood, Clarendon Press, Oxford, pp. 21-42, 1993.
3. J. Bonel and R.D. Wood, in Mathematical Modeling for Materials Processing, ed. M. Cross, J.F.T. Pittman, and R.D. Wood, Clarendon Press, Oxford, pp. 137-158, 1993.
4. F.R. Hall, P. Hartley, I. Pillinger, C. Sturgess, A.V. Bael, P.V. Houtte, and E. Aernoudt, in Mathematical Modeling for Materials Processing, ed. M. Cross, J.F.T. Pittman, and R.D. Wood, Clarendon Press, Oxford, pp. 177-194, 1993.
5. R.B. Thompson, E.P. Papadakis, D.D. Bluhm, G.A. Alers, K. Forouraghi, H.D. Skank, S.J. Wormley, in J. Nondest. Eval., 1993, 12(1), 45.
6. A.J. Anderson, Ph.D. Thesis, 1997, (Iowa State University).
7. L.L. Dillamore and W.T. Roberts, Metallurgical Review, 1965, Vol. 10, No. 39, pp270-380.
8. R.O. Williams, Tran. Metall. Sci. AIME, 1968, Vol.242, p105.
9. R.J. Roe, J. Appl. Phys., 1965, Vol.36, p2024.
10 R.B. Thompson, J.F. Smith, S.S. Lee and G.C. Johnson, Metall. Trans., 20A, 2431(1989).
11. W.Y. Lu, J.G. Morris and Q. Gu, QNDE, 1991, 10B, p1983.
12. C.M. Sayers, J. Phys. D: Appl. Phys., 1982, Vol.15, p2157.
13. R.B. Thompson, S.S. Lee, and J.F. Smith, J. Accoust. Soc. Am 80(3), 1986.
14. Y. Li, R.B. Thompson, and S.J. Wormley, QNDE, 1991, 10B, p1991.
15. K. Forouraghi, R.B. Thompson, A.J. Anderson, N. Izworski, M. Shi, F. Reis, and J. Roo, QNDE, 1996, 15B, p1621.
16. G. Simmons, and H. Wang, Single Crystal Elastic Constants and Calculated Aggregate Properties: A HANDBOOK, The MIT Press, 1971.
17. S.I. Wright, J. Computer-Assisted Microscopy, Vol. 5, No.3, 1993, p 207.
18. M. Stout, Los Alamos National Laboratory, private communication.
19. A.J. Anderson, R.B. Thompson, R. Bolingbroke, and J.H. Root, Textures and Microstructures, 1996, Vol. 26-27, pp. 39-58.